UNIVERSIDADE ESTADUAL PAULISTA
"JÚLIO DE MESQUITA FILHO"
Instituto de Biociências
Câmpus do Litoral Paulista

LUISA TROVATTI CUSTÓDIO

MORPHOLOGY AND HISTOLOGY OF THE OLFACTORY ROSETTE OF THE LESSER-SPOTTED DOGFISH, *SCYLIORHINUS CANICULA* (CHONDRICHTHYES, SCYLIORHINIDAE)

São Vicente - SP
2026

Instituto de Biociências - Câmpus do Litoral Paulista
Praça Infante D. Henrique s/nº - CEP 11330-900 - São Vicente (SP) - Brasil
Tel. (13) 3569-7100 – email diretor.clp@unesp.br

UNIVERSIDADE ESTADUAL PAULISTA
"JÚLIO DE MESQUITA FILHO"
Instituto de Biociências
Câmpus do Litoral Paulista

LUISA TROVATTI CUSTÓDIO

MORPHOLOGY AND HISTOLOGY OF THE OLFACTORY ROSETTE OF THE LESSER-SPOTTED DOGFISH, *SCYLIORHINUS CANICULA* (CHONDRICHTHYES, SCYLIORHINIDAE)

Trabalho de conclusão de curso apresentado à Universidade Estadual Paulista (UNESP), Instituto de Biociências, Campus do Litoral Paulista, como parte dos requisitos para obtenção do Grau de bacharel em Ciências Biológicas, com habilitação em Gerenciamento Costeiro.

Orientador: Otto Bismarck Fazzano Gadig

São Vicente - SP
2026

C987m

Custódio, Luisa Trovatti

Morphology and histology of the olfactory rosette of the lesser-spotted dogfish, Scyliorhinus canicula (Chondrichthyes, Scyliorhinidae) / Luisa Trovatti Custódio. -- São Vicente, 2026

28 p. : il., tabs., fotos

Trabalho de conclusão de curso (Bacharelado - Ciências Biológicas) - Universidade Estadual Paulista (UNESP), Instituto de Biociências, São Vicente

Orientador: Otto Bismarck Fazzano Gadig

1. Elasmobranchs. 2. Olfaction. 3. Secondary folds. I. Título.

Sistema de geração automática de fichas catalográficas da Unesp. Dados fornecidos pelo autor(a).

Morphology and histology of the olfactory rosette of the lesser-spotted dogfish, *Scyliorhinus canicula* (Chondrichthyes, Scyliorhinidae)

Luisa Trovatti Custódio[a,b], Sara Ferrando[c] & Otto Bismarck Fazzano Gadig[a,b]

[a] São Paulo State University (UNESP), Institute of Biosciences - Praça Infante Dom Henrique, s/n - Parque Bitaru, São Vicente, SP, 11330-900, Brazil.

[b] Laboratory of Elasmobranch Research (ELASMOBRASIL) - São Paulo State University (UNESP), Institute of Biosciences, São Vicente, SP, 11330-900, Brazil. E-mail: (LTC) luisa_trovatti@hotmail.com; (OBFG) otto.gadig@unesp.br.

[c] Department of Earth, Environmental, and Life Sciences (DISTAV), University of Genoa (UniGe) - Corso Europa, 26, 16132 Genoa, Italy. E-mail: (SF) sara.ferrando@unige.it.

Corresponding Author: Luisa Trovatti Custódio: luisa_trovatti@hotmail.com

ORCID: LTC (0009-0009-9522-2530); OBFG (0000-0002-8109-5085); SF (0000-0002-5781-9709).

Running Head: Functional characterization of the olfactory rosette.

Acknowledgments

We thank the *Fundação de Amparo à Pesquisa do Estado de São Paulo* (FAPESP) for the undergraduate fellowship granted to LTC (#2024/08775-6 and #2024/23384-3) and we also thank the Department of Earth, Environmental, and Life Sciences (DISTAV) for all the infrastructure.

Funding

This work was financially supported by FAPESP under grant (#2024/23384-3).

Abstract

The study of the sensory organs of a species improves the understanding of its behavior and ecology. Elasmobranch fishes occupy a wide range of ecological niches, and several aspects of their biology are still largely unknown. The sense of smell may have different levels of importance among species. This study investigated the morphology and histology of the olfactory rosette of the lesser-spotted dogfish (*Scyliorhinus canicula*). The research was conducted at the Dipartimento di Scienze della Terra, dell'Ambiente e della Vita (DISTAV), Università di Genova, under the supervision of PhD Sara Ferrando. Four adult specimens of *S. canicula* were collected and measured. The olfactory organ of this species, as in other elasmobranchs, is a rosette characterized by the presence of primary lamellae (macroscopically visible) and secondary folds (microscopical visible). Morphometric data were obtained from the olfactory rosettes using a caliper, and three primary lamellae representing different regions of each rosette were removed for surface area measurements using ImageJ software. In addition, the rosettes underwent histological processing to estimate, using ImageJ software on micrographs, the contribution of the secondary folds to the sensory surface area, thereby enabling the calculation of the olfactory capacity of each specimen. The specimens (TL ranging from 41.9 to 48.2 cm) had a sensory surface area ranging from approximately 10 to 19 cm^2 when only primary lamellae were considered and from 40 to 134 cm^2 when the secondary folds were included. These results indicate that the contribution of the secondary folds to the surface area increases as the fish grows. The data obtained provide valuable insights into the sensory abilities of a medium-sized coastal predator that plays a key ecological role.

Keywords: elasmobranchs; olfaction; secondary folds.

1. Introduction

Sharks (Class Chondrichthyes; Subclass Elasmobranchii) possess a highly developed array of sensory systems [1, 2] that enable them to detect prey and conspecifics, avoid predators and obstacles, and navigate through their environment [3]. Consequently, many species are considered apex predators within food webs and play a key role in regulating ecosystem function [4]. They occupy a wide range of ecological niches in aquatic environments, particularly in marine environments [5, 6, 7]. Each sensory modality enables the perception of specific environmental cues, including light, chemicals, mechanical stimuli, and electric fields, across different spatial scales and sensitivity levels [4]. Understanding the evolutionary diversification of these sensory systems is therefore essential for explaining how environmental information is processed, which often requires a multi-level approach encompassing genes, cells, and organs [8].

In this context, research on the olfactory organs of Chondrichthyes has grown considerably [3, 9], highlighting their crucial contribution to the overall sensory repertoire of cartilaginous fishes [1, 2, 10, 11, 12, 13, 14, 4, 3, 15]. These structures are vital for key survival functions such as prey detection, predator avoidance, and chemosensory communication with conspecifics [16, 1, 17, 18, 12, 13, 4, 3, 15]. As a result, they contribute significantly to a more accurate ecological understanding of these species [19].

In elasmobranchs, the peripheral olfactory system is generally characterized by a multilamellar olfactory organ, the olfactory rosette, covered by sensory and non-sensory epithelia that respond to specific odor molecules in the aquatic environment [20, 21, 22].

The olfactory organs are located on the lateral–ventral aspect of the head, close to the mouth, within laterally positioned cartilaginous capsules [23, 12, 3]. They communicate with the external environment through paired nostrils, which are typically divided by skin-covered flaps into a lateral incurrent naris and a medial excurrent naris [23, 24, 25, 3]. Water enters the olfactory capsule through the incurrent naris, flows over the olfactory

lamellae, and exits through the excurrent naris [24, 25, 26, 3, 27, 28, 22].

Inside the olfactory capsule lies the olfactory sac, which is almost entirely occupied by the olfactory rosette. The rosette consists of two rows of stacked, wing-shaped lamellae that originate from a central ridge, the raphe, and attach to the wall of the olfactory cavity [23, 24, 25, 29, 13, 3, 22].

The morphology of the olfactory rosette varies substantially among elasmobranch species, this variation includes rosette size and shape, positioning of the nares, number of lamellae, lamellar surface area, and sensory epithelial surface area [23, 30, 31, 32, 33, 24, 25, 34, 35, 29, 36, 37, 13, 3, 38, 15]. Depending on the species, lamellae may extend perpendicular to the raphe or be arranged radially around a central axis [39, 21, 40, 36, 13, 22]. Each lamella bears secondary folds that greatly increase the surface area of the olfactory epithelium, which is divided into sensory and non-sensory regions [12, 3].

Scyliorhinus canicula is an extremely common shark along the northeastern Atlantic coast, with a distribution extending from Senegal to southern Norway [41]. It also occurs in the Mediterranean and Adriatic Seas [42]. This species primarily inhabits sandy, gravelly, or muddy bottoms at depths ranging from a few meters to approximately 400 m [43, 44, 45, 42] In the Cantabrian Sea, its distribution is continuous along the continental shelf, although individuals may aggregate according to sex and size. Juveniles are predominantly found in the eastern region at depths around 200 m, whereas adults occur over a broader depth range (50-450 m), most commonly between 150 and 300 m [46, 47, 48, 42]. The diet consists mainly of benthic organisms, including crustaceans, mollusks, and small teleost fishes [49]. Like all members of the family Scyliorhinidae, *S. canicula* is oviparous [50, 51].

Based on the above, this study aimed to describe the morphology of the olfactory rosette, correlate body and olfactory rosette morphometric variables, and characterize the olfactory epithelium through histological analyses. The surface area of the primary

lamellae and secondary folds was quantified using ImageJ to estimate the olfactory capacity of the lesser-spotted dogfish, *Scyliorhinus canicula*.

2. Material and Methods

2.1. Precedence and morphology analysis

The four specimens analyzed were obtained from accidental bycatch captured by professional fishermen in the Ligurian Sea, Northwestern Mediterranean. The samples were collected onboard, fixed in 4% paraformaldehyde in 0.1 M phosphate-buffered saline (PBS, pH 7.4), washed in PBS, and stored in 70% ethanol. Each specimen was photographed from dorsal, ventral, and lateral views.

The following data were collected, adapted from Timm & Fish (2012): sex, sexual maturity, total length, head length and width, total nostril length, incurrent nostril length, nasal lobe length, internasal distance, pre-nasal distance, nose-mouth distance, pre-oral distance, mouth length and width, and horizontal eye diameter (Figures 1 and 2). These measurements were used to determine whether there is any correlation between the morphology of the body and that of the olfactory rosette.

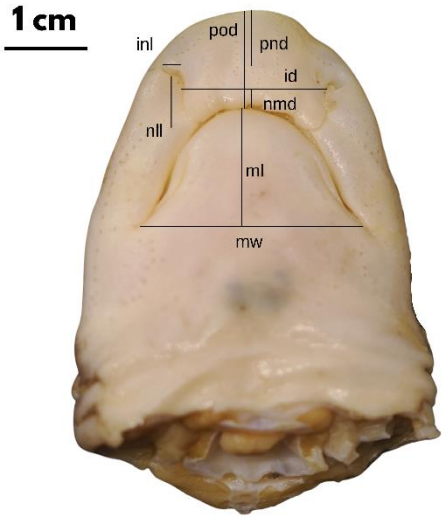

Figure 1. Ventral view of the head of the lesser-spotted dogfish, showing the morphometric data taken. Abbreviations: inl = incurrent nostril length; nll = nasal lobe length; id = internasal distance; pnd = pre-nasal distance; nmd = nasal-mouth distance; pod = pre-oral distance; ml = mouth length; mw = mouth width.

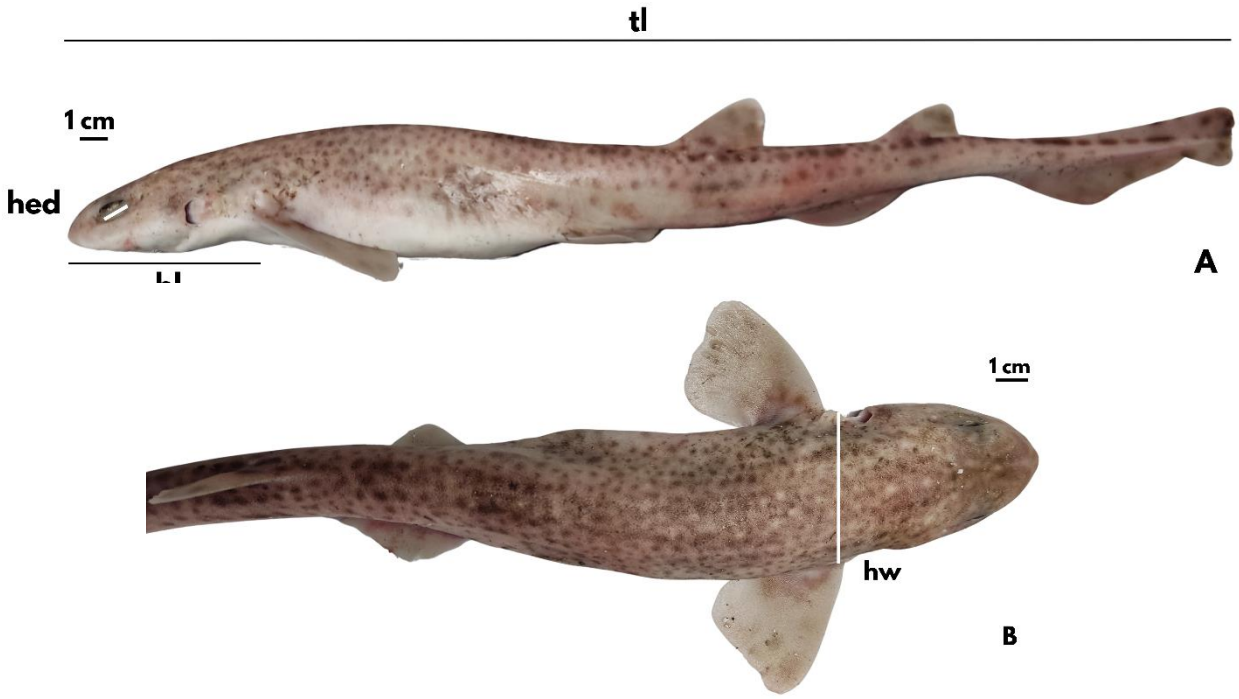

Figure 2. Lateral (A) and dorsal (B) views of the lesser-spotted dogfish, showing the morphometric data taken. Abbreviations: tl = total length; hed = horizontal eye diameter; hl = head length; hw = head width.

The olfactory rosette from the left nostril of each specimen was removed by manual dissection using a scalpel and then photographed. The following parameters were recorded: length, width, and volume. The length and width of the rosette were measured using an analog caliper (Figure 3), and its volume was determined by immersion in a graduated cylinder. The proportional dimensions of the length and width of the olfactory rosette were compared with the previously described morphometric variables of the body. The terminology used for the structures composing the olfactory rosette follows that commonly employed in similar anatomical studies [29, 37, 52, 19].

Figure 3. The olfactory rosette of the lesser-spotted dogfish, showing the morphometric data taken with the analog caliper. Abbreviations: rl = rosette length; rw = rosette width.

The olfactory rosette was bisected, with one half reserved for morphometric analysis, and the other for histological processing. Three primary lamellae were manually dissected from each olfactory rosette using a scalpel: one from one end, one from the middle, and one from the opposite end of the selected half. This sampling strategy was designed to account for regional variation in lamellar morphology across the olfactory rosette.

2.2. Histology and characterization of the olfactory epithelium

Following the methodology of [52], the other half of the olfactory rosette was processed for histological investigation of the secondary folds. Tissue samples were embedded in paraffin according to the following protocol: 2 h in 80% EtOH, 2 h in 90% EtOH, 8 h in 95% EtOH, 1 h in 100% EtOH (I), 1 h in 100% EtOH (II), 1 h in 100% EtOH (III), 15 min in 50% EtOH + 50% Bioclear, 3 min in Bioclear (I), 3 min in Bioclear (II), 3 min in Bioclear (III), 15 min in Bioclear + paraffin in an oven at 60ºC, 1 h in paraffin (I), 1 h in paraffin (II), and 1 h in paraffin (III).

After embedding, the material was blocked and sectioned at a thickness of 5 μm using a microtome. As a standard procedure, 1.000 μm were discarded between each section, except in specific cases described below. Approximately 20 to 25 slides were prepared for each specimen, each containing about four to six slices.

2.2.1. Hematoxylin and Eosin (BIOPTICA) staining

Hematoxylin is a basic dye that stains nuclei and other basophilic components violet, while Eosin is an acidic dye that stains the cytoplasmic and other acidophilic elements pink. This staining was first applied in three or four slides selected to represent the entire structure.

For specimen 24.1, slides #8, #13, and #25 were selected. For slide #25, an interval of 2.000 μm was discarded from the previous section, as the raphe level had not yet been reached. For specimen 24.2, slides #6, #16, #21, and #24 were chosen, with 1.040 μm discarded before slide #24 for the same reason. For specimen 24.3, slides

#3, #7, #15, and #19 were selected; between slides #15 and #19, 2.000 μm were discarded due to a small cartilage fragment that was damaging the tissue and required removal. For specimen 24.4, slides #8, #17, and #20 were selected.

For staining, the samples underwent paraffin removal and rehydration as follows: 15 min in Bioclear (I), 15 min in Bioclear (II), 1 min in 100% EtOH (I), 1 min in 100% EtOH (II), 1 min in 95% EtOH, 1 min in 90% EtOH, 1 min in 80% EtOH, and finally rinsed in distilled water.

The coloration procedure consisted of 6 min in Hematoxylin, 10 min in tap water, 1 min in distilled water, 6 min in Eosin, and 5 min in distilled water. For dehydration and clearing, the slides were processed sequentially for 5–10 s in 80%, 90%, 95%, 100% EtOH (I), and 100% EtOH (II), followed by 1 min in Bioclear (I) and Bioclear (II).

To prepare the slides for microscopic analysis, a coverslip was carefully positioned, and the slides were dried in an oven for 24 hours. After drying, they were observed under the microscope, and between three and five secondary folds were selected to measure both their linear length and total length.

2.2.2. Alcian Blue PAS + Gill's Hematoxylin (Sigma-Aldrich) staining

The Alcian Blue PAS + Gill's Hematoxylin technique was used to identify and differentiate mucopolysaccharides in the olfactory epithelium. Alcian Blue stains acidic mucopolysaccharides blue, while PAS (Periodic Acid–Schiff) stains neutral mucopolysaccharides pink. Gill's Hematoxylin was used as a nuclear counterstain.

This staining was performed on one slide from each specimen. For specimen 24.1, slide #20 was selected; for specimen 24.2, slide #17; for specimen 24.3, slide #17, with 2.000 μm discarded from the last section due to a small cartilage fragment that was damaging the tissue and required removal; and for specimen 24.4, slide #5. Paraffin removal and rehydration were carried out following the same procedure

previously described for Hematoxylin and Eosin staining. The staining protocol consisted of 5 min in Alcian Blue, 3 min in tap water, 3 min in distilled water, 5 min in Periodic Acid, 3 min in distilled water, 15 min in Schiff reagent, 5 min in tap water, 90 s in Gill's Hematoxylin, 3 min in tap water, and 3 min in distilled water.

Dehydration and clearing were performed as described in section 3.2.1. Finally, a coverslip was applied, and the slides were dried in an oven for 24 hours before microscopic observation.

2.2.3. Azan Trichrome (BIOPTICA) staining

Azan Trichrome staining was used as the method of choice for connective tissue analysis. The procedure was performed on one slide from each specimen. For specimen 24.1, slide #24 was selected, with 2.000 μm discarded from the last section, as the raphe level had not yet been reached. For specimen 24.2, slide #15 was used; for specimen 24.3, slide #18, with 2.000 μm discarded from the last section due to the presence of a small cartilage fragment that was damaging the tissue and required removal; and for specimen 24.4, slide #4.

Paraffin removal and rehydration were carried out following the same procedure described for Hematoxylin and Eosin staining. The staining protocol consisted of the following steps: Solution A (Azocarmine according to Heidenhain): 30 minutes in a humid chamber in an oven at 56 °C, followed by 5 min at room temperature; excess was removed by dripping; Solution B (Alcohol-aniline): 1 min, followed by removal of excess; Solution C (Acidified alcohol, stopping solution): 1 min, then excess removed; Solution D (Phosphotungstic acid solution): 30 min in a humid chamber, excess removed afterward; Solution E (Polychrome mixture according to Mallory): 30 min in a humid chamber, followed by a brief wash (maximum 30 s) in 95% EtOH. Dehydration and clearing followed the protocol described in section 3.2.1. Finally, a coverslip was carefully positioned, and the slides were dried in an oven for 24 hours

prior to microscopic analysis.

2.2.4. Sirius Red (Sigma-Aldrich) staining

Sirius Red staining was used to observe collagen presence in the tissue, allowing color differentiation among fiber types. The thinnest fibers ranged in color from yellow to green, whereas thicker fibers appeared red. Observation was performed under polarized light using two filters, which rendered the background (non-collagenous tissue) black, leaving only the fibers visible. Because the collagen structure disrupts the orientation of polarized light, the fibers appear bright under the microscope.

The Picrosirius solution contained 0.1 g of Sirius Red dissolved in 100 mL of a saturated picric acid solution, and the 0.5% acetic acid solution was prepared by adding 50 μL of glacial acetic to 10 mL of distilled water.

The procedure was performed on one slide from each specimen. For specimen 24.1, slide #15 was selected; for specimen 24.2, slide #22, with 1.040 μm discarded from the last section due to the presence of a small cartilage fragment that was damaging the tissue and required removal; for specimen 24.3, slide #14; and for specimen 24.4, slide #1. Paraffin removal and rehydration were carried out following the same procedure described for Hematoxylin and Eosin staining.

The staining protocol consisted of 1 h in Picrosirius solution in a humid chamber, after which the excess solution was removed by dripping. The slides were then washed twice with 0.5% acetic acid, and excess solution was again removed by dripping.

Dehydration and clearing were performed more rapidly than described in section 3.2.1, with 5–10 seconds in 100% EtOH (I) and 100% EtOH (II). Finally, a coverslip was carefully positioned, and the slides were dried in an oven for 24 hours prior to microscopic analysis.

2.3. Calculations of the analysis of the olfactory capability

All samples were examined using a Leica DMRB light microscope, and images were captured with a Leica CCD camera DFC420C (Leica, Switzerland) [53]. Image analysis was performed with ImageJ Software [54, 55, 37, 19, 52].

To calculate the olfactory capability of this species, the average area of the three lamellae was determined and multiplied by twice the total number of lamellae, accounting for both surfaces of each lamella. This provided the total surface area of the primary lamellae in one olfactory rosette. To obtain a more accurate estimate, the presence of secondary folds containing sensory epithelium was also considered. The calculation was performed as follows: the length of the secondary folds (L2) was multiplied by 100 and divided by the linear length of the lamella (L1), yielding the approximate percentage of surface area (referred to as X). This procedure was repeated for three to five lamellae, and the average of these values was calculated (referred to as Y). The Y value was then multiplied by the total surface area of the primary lamellae and divided by 100, resulting in the final olfactory capability value for each specimen.

By combining the surface area of the primary lamellae with the proportional increase contributed by the secondary folds, this method provides a more accurate estimation of the total sensory epithelial surface and, consequently, of the olfactory capability of the specimen (Figure 4).

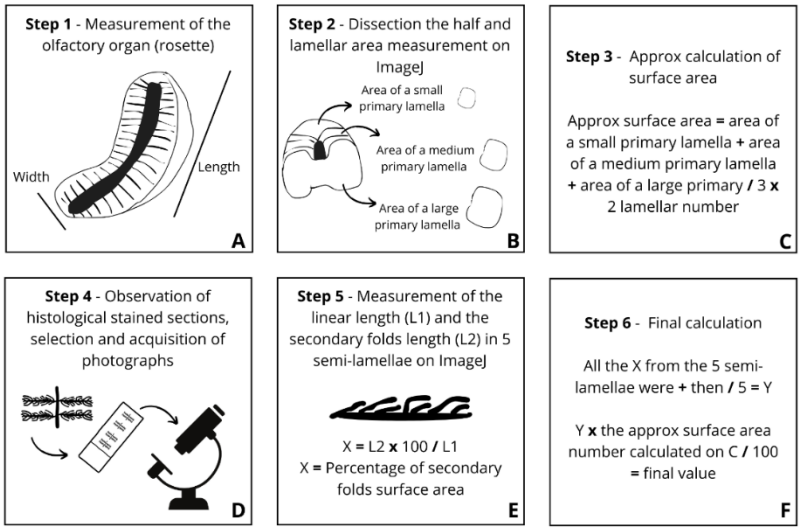

Figure 4. Diagram illustrating the process used to obtain the measurements analyzed in this study. (A) Measurements as length, width and volume (not shown in the figure) were taken from the olfactory organ (rosette) of four specimens of the lesser-spotted dogfish, each exhibiting an elongated raphe. (B) The half of the olfactory organs were dissected to obtain three lamellae of different sizes (one small, one medium and one large) for surface area calculation. (C) Calculation used to estimate a proxy for the gross surface area of the organs. (D) The olfactory organs were processed using standard histological methods, observed, and photographed under a stereomicroscope. (E) The linear length and the corresponding boundary with secondary folds of five primary lamellae were measured to calculate the percentage of surface increase due to the secondary folds. (F) Calculation used to estimate the final value of the olfactory capability of the specimens. (Adapted from Ferrando *et al*., 2019).

To quantify the amount of collagen within a given area, Sirius Red staining was employed. Two images were selected: one representing tissue with abundant dense collagen and another showing tissue with lower collagen content composed of thinner fibers. For both images, the color threshold was adjusted to a brightness range of 50–255 using ImageJ Software on the polarized light micrographs. Three rectangular regions were selected in each image, and the total area in pixels and mean gray value were measured. Using equations in Microsoft Excel, the number of black pixels was calculated as the total area in pixels multiplied by ((mean gray – 255) / –255), while the number of white pixels was obtained by subtracting the black pixel value from the total area. The percentage of collagen was then determined as (white pixels × 100) divided by the total area in pixels. Finally, the average collagen percentage was calculated separately for the thin-fiber and thick-fiber tissue samples.

2.4. Statistical analysis

Statistical analysis was conducted in the R 4.3.0 environment (R Core Team, 2023). Prior to the analyses, data normality was tested using the Shapiro-Wilk test. The morphometric data of the body and the internal nasal morphology of each *Scyliorhinus canicula* specimen were then correlated using the Pearson correlation coefficient for variables with $p > 0.05$ in the Shapiro–Wilk test, and the Spearman correlation coefficient for variables with $p < 0.05$ in the same test. The significance level for all correlations was set at $\alpha = 0.05$. For the semi-quantitative analysis of collagen, data normality was initially tested using the Shapiro–Wilk test. Subsequently, an ANOVA was performed, considering a significance level of $\alpha = 0.05$.

In addition, a descriptive analysis was performed for the four specimens, calculating the minimum, maximum, mean, and standard deviation values for all variables (morphometric variables of the body and the olfactory organ).

3. Results

3.1. Morphological analysis and calculation of olfactory capacity

Regarding the external morphology, it was observed that the rostrum of the lesser-spotted dogfish is slightly pointed. The olfactory organ is located ventrolaterally on the snout, close to the mouth. A distinct feature observed is that, from the anterior margin, a large nasal flap extends toward the mouth, partially covering the excurrent nostril. The incurrent nostril is circular, whereas the excurrent nostril is oval and considerably smaller. The olfactory organ is enclosed within a thin cartilaginous nasal capsule. The olfactory rosette is slightly elongated and consists of two rows of lamellae separated by a slightly curved transverse raphe.

Inside the olfactory rosette, the lamellae are arranged such that they are largest in the middle of the organ and gradually decrease in size toward both ends. According to the literature, *Scyliorhinus canicula* has approximately 33 lamellae in the olfactory rosette [56]. Each lamella bears secondary folds (Figure 5), which significantly increase the surface area of the olfactory organ, as indicated by the data collected (Table 1).

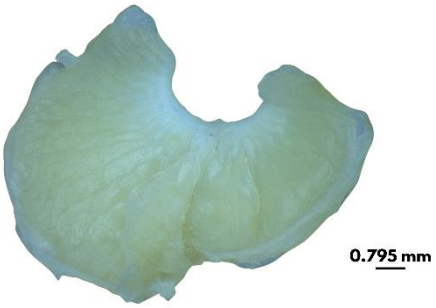

Figure 5. In this figure, it is possible to see the two wing-shaped lamellae from the olfactory organ of the lesser-spotted dogfish.

Table 1. Data of *Scyliorhinus canicula* specimens analyzed in this study. All specimens were collected from the Ligurian Sea, Northwestern Mediterranean, on 28 May 2024.

Parameter	24.1	24.2	24.3	24.4
Sex	Male	Female	Female	Male

Maturity	Adult	Pregnant adult	Adult	Adult
Conservation	Fixed	Fixed	Fixed	Fixed
Institution	DISTAV	DISTAV	DISTAV	DISTAV
Total length (cm)	41.90	43.20	42.70	48.20
Head length (cm)	7.56	6.93	6.66	8.61
Head width (cm)	4.07	4.17	5.08	5.04
Nostril length (cm)	0.80	0.81	0.90	0.90
Incurrent nostril length (cm)	0.24	0.29	0.30	0.35
Nasal lobe length (cm)	0.72	0.62	0.88	0.98
Internasal distance (cm)	1.81	1.80	1.80	2.10
Prenasal distance (cm)	0.80	1.10	0.90	1.60
Nose–mouth distance (cm)	0.29	0.31	0.40	0.45
Preoral distance (cm)	1.25	1.60	1.70	2.00
Mouth length (cm)	1.49	1.50	1.50	1.95
Mouth width (cm)	2.90	2.80	3.10	3.35
Horizontal eye diameter (cm)	1.20	1.30	1.10	1.20
Rosette volume (ml)	0.30	0.40	0.20	0.50
Rosette length (cm)	1.38	1.42	1.49	1.65
Rosette width (cm)	0.80	0.91	0.96	1.23
Large primary lamella area (cm^2)	0.203	0.256	0.267	0.341
Medium primary lamella area (cm^2)	0.140	0.181	0.183	0.316
Small primary lamella area (cm^2)	0.100	0.168	0.133	0.263
Average lamelar area (cm^2)	0.148	0.202	0.194	0.306
Average * twice number lamellae (cm^2)	9.746	13.310	12.826	19.470
Average linear length (cm)	0.259	0.319	0.312	0.376
Average secondary folds length (cm^2)	1.116	1.834	1.480	2.704
% of increase	416.01	564.6	475.22	689.83
Total surface	40.54	75.15	60.95	134.31

area (cm^2)

Furthermore, a descriptive analysis (minimum, maximum, mean, and standard deviation) was performed for 17 morphometric data obtained from the four specimens of *Scyliorhinus canicula* (Table 2). It is possible to observe that the other parameters follow a growth pattern consistent with total length.

Table 2. Descriptive analysis including minimum, maximum, mean, and standard deviation of 17 morphometric data of four specimens of *Scyliorhinus canicula*.

Parameter	Min	Max	Mean ± SD
Total length (cm)	41.9	48.2	44 ± 2.85
Head length (cm)	6.66	8.61	7.44 ± 0.87
Head width (cm)	4.07	5.08	4.59 ± 0.54
Mouth lenght (cm)	1.49	1.95	1.61 ± 0.23
Mouth width (cm)	2.8	3.35	3.04 ± 0.24
Nasal slit length (cm)	0.8	0.9	0.85 ± 0.06
Incurrent nostril length (cm)	0.24	0.35	0.3 ± 0.05
Nasal lobe length (cm)	0.62	0.98	0.8 ± 0.16
Internasal distance (cm)	1.8	2.1	1.9 ± 0.15
Preoral distance (cm)	1.25	2	1.64 ± 0.31
Prenasal distance (cm)	0.8	1.6	1.1 ± 0.36
Nose-mouth distance (cm)	0.29	0.45	0.36 ± 0.08
Horizontal eye diameter (cm)	1.1	1.3	1.2 ± 0.08
Rosette surface area (cm^2)	40.54	134.31	77.74 ± 40.3

Rosette length (cm)	1.38	1.65	1.49 ± 0.12
Rosette width (cm)	0.8	1.23	0.98 ± 0.18
Rosette volume (ml)	0.2	0.5	0.35 ± 0.13

In addition, the body variables were correlated with the rosette variables (Table 3). Significant correlations were observed for the following parameters: total length (cm) with rosette surface area (cm^2) and rosette volume (mL); incurrent nostril length (cm) with rosette width (cm); pre-oral distance (cm) with rosette width (cm); pre-nasal distance (cm) with rosette surface area (cm^2); and nose–mouth distance (cm) with rosette length (cm).

Table 3. Correlation values (Pearson and Spearman) for each body measurement with the rosette measurements. cor = Pearson's correlation coefficient. rho = Spearman's correlation coefficient. p = Significance of the correlation, with α being set to 0.05. Significant correlations are marked with an asterisk *.

	Rosette surface area (cm^2)		**Rosette length (cm)**		**Rosette width (cm)**		**Rosette volume (ml)**	
Measurements	**cor/rho**	**p**	**cor/rho**	**p**	**cor/rho**	**P**	**cor/rho**	**P**
Total length (cm)	0.99/-	0.01*	0.94/-	0.06	0.97/-	0.03*	0.81/-	0.19
Head length (cm)	-/0.4	0.75	0.68/-	0.32	0.76/-	0.24	0.78/-	0.22
Head width (cm)	0.57/-	0.43	0.82/-	0.18	0.68/-	0.32	-0.01/-	1
Mouth length (cm)	0.94/-	0.06	0.93/-	0.07	0.94/-	0.06	0.77/-	0.23
Mouth width (cm)	0.76/-	0.24	0.94/-	0.06	0.89/-	0.11	0.35/-	0.65
Nasal slit length (cm)	0.59/-	0.41	0.83/-	0.17	0.77/-	0.23	0.02/-	0.98

Incurrent nostril length (cm)	0.93/-	0.07	0.94/-	0.06	0.97/-	0.03*	-/0.4	0.75
Nasal lobe length (cm)	0.63/-	0.37	0.87/-	0.13	0.8/-	0.2	0.16/-	0.84
Internasal distance (cm)	0.93/-	0.07	0.91/-	0.09	0.91/-	0.08	0.77/-	0.23
Preoral distance (cm)	0.91/-	0.09	0.94/-	0.06	0.95/-	0.05*	-/0.4	0.75
Prenasal distance (cm)	0.99/-	0.01*	0.89/-	0.11	0.94/-	0.06	0.87/-	0.13
Nose-mouth distance (cm)	0.78/-	0.22	0.95/-	0.05*	0.92/-	0.08	0.29/-	0.71
Horizontal eye diameter (cm)	0.14/-	0.86	-0.24/-	0.76	-0.11/-	0.89	-/0.63	0.37

These results may be explained by two possible factors: first, the small sample size may not have provided sufficient data to establish reliable correlations among the measurements; second, since the four specimens were approximately the same size, there was little variation to encompass a broader ontogenetic range.

3.2. Histological analyses and characterization of the olfactory epithelium

The olfactory lamella is covered by both sensory and non-sensory epithelium. It consists of three main cell types present: basal cells located on the bottom, receptor cells with the nuclei located in the middle, and supporting cells with the nuclei at the apical surface, where microvilli are present along with cilia as, receptor cells have microvilli, while the supporting cells are ciliated. Along the epithelium, the presence of mucous cells was also observed (Figure 6).

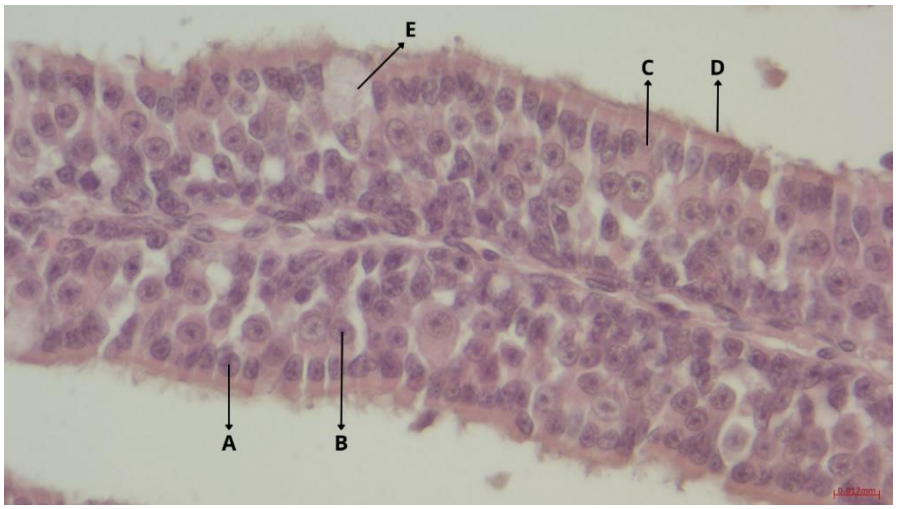

Figure 6. Olfactory epithelium of *Scyliorhinus canicula* in Hematoxylin and Eosin staining. (A) Basal cells; (B) Receptor cells; (C) Supporting cells; (D) Microvilli; (E) Mucous cell.

Using the Alcian Blue PAS + Gill's Hematoxylin staining, it was possible to observe and differentiate the elongated mucous cells (Figure 7). The mucous cells located in the non-sensory epithelium which lines internally the connective olfactory capsule, exhibited a more bluish coloration, whereas those present in the olfactory epithelium of the secondary folds showed a purplish tone. This difference may be related to the type of mucous cell, the cells within the olfactory capsule may be less acidic than those in the olfactory epithelium of the secondary folds.

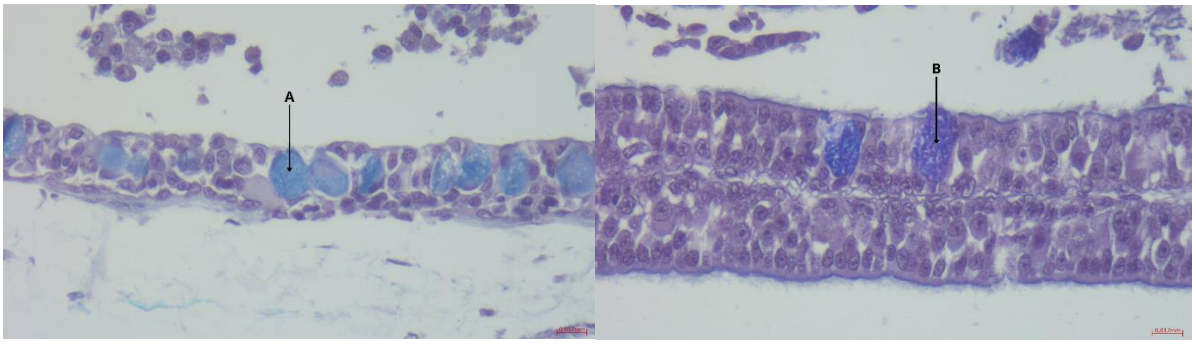

Figure 7. Mucous cells of *Scyliorhinus canicula* stained with Alcian Blue PAS + Gill's Hematoxylin. (A) Mucous cells located in the epithelium covering the connective olfactory capsule; (B) Mucous cells located in the olfactory epithelium of the secondary folds.

Using Azan Trichrome staining, it was possible to observe the connective tissue (Figure 8). The basal lamina appeared more intensely stained and thicker in the center of the raphe and in areas with denser connective tissue. In contrast, the basal lamina was less

stained and much thinner in regions such as at the extremities of the secondary folds.

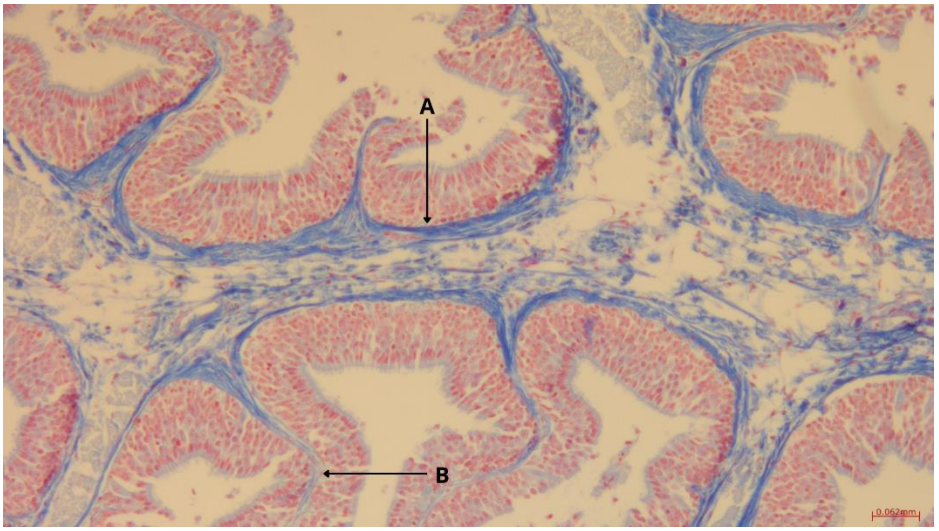

Figure 8. Olfactory epithelium of *Scyliorhinus canicula* stained with Azan Trichrome. (A) Thick basal lamina; (B) Thin basal lamina.

Finally, through Sirius Red staining, it was possible to observe that collagen distribution within the olfactory rosette is not uniform (Figure 9). The collagen fibers appeared denser and more abundant in regions where the tissue is more rigid, such as the raphe, whereas thinner and less abundant collagen fibers were found in softer tissue areas. This difference may be related to the water flow through the incurrent and excurrent chambers, in regions where the water flows more strongly, such as the raphe, the tissue needs to be more resistant to pressure, thus containing more collagen. In contrast, water flows more gently through the secondary folds, allowing these regions to have less structural reinforcement and consequently less collagen.

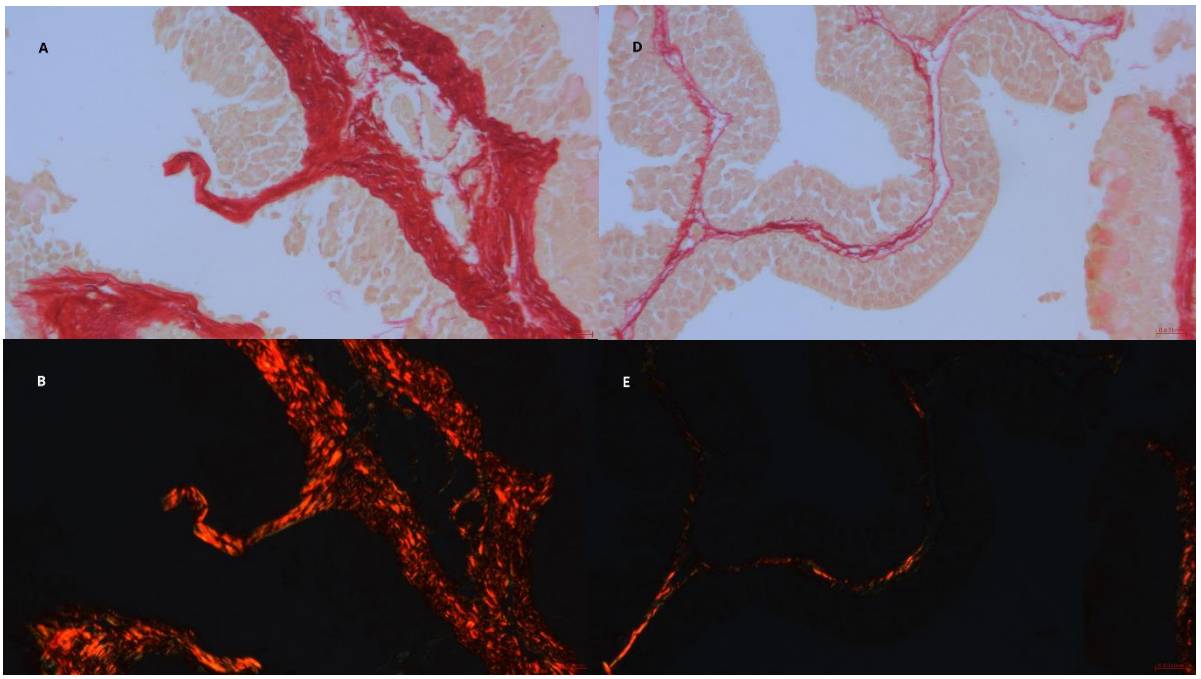

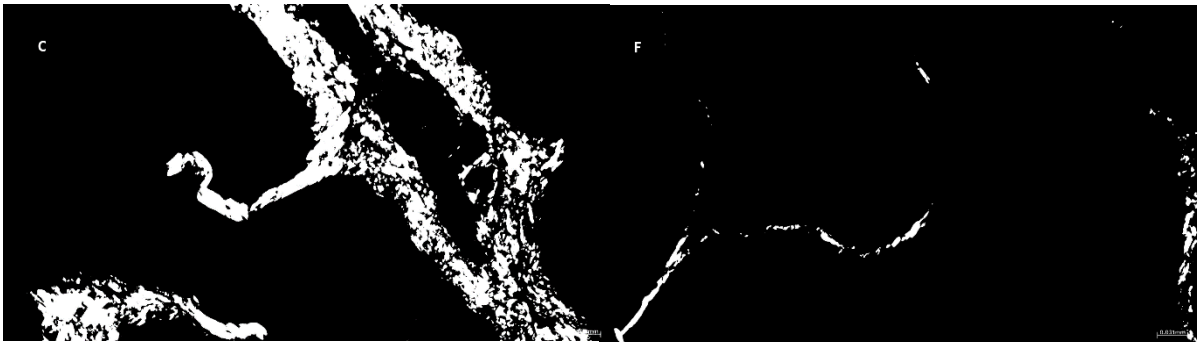

Figure 9. Sirius Red staining of *Scyliorhinus canicula.* (A) Region with abundant collagen and dense collagen fibers observed under the stereomicroscope, (B) under two polarized light filters; (C) analyzed in ImageJ Software using a 50–255 brightness range for the black-and-white threshold; (D) Region with less collagen and thinner fibers observed under the stereomicroscope; (E) under two polarized light filters; (F) analyzed in ImageJ Software using a 50–255 brightness range for the black-and-white threshold.

According to the results of the semi-quantitative collagen analysis (Table 4), there was a significant difference ($p = 0.001$) between thin and thick collagen in the olfactory lamellae. Overall, all specimens showed a higher percentage of thick collagen compared to thin collagen (Figure 10). This may occur because only in the secondary folds is the tissue softer, as water flows through these regions with lower pressure. In contrast, in other areas of the olfactory organ, where water flow is stronger, the tissue presents denser collagen fibers.

Table 4. Semi-quantitative analysis of collagen in the olfactory rosette of four specimens of *Scyliorhinus canicula.*

Specimen	Thin collagen (%)	Thick collagen (%)
24.1	31.4	74.15
24.2	27.6	71.24
24.3	41.94	70.34
24.4	54.88	77.75

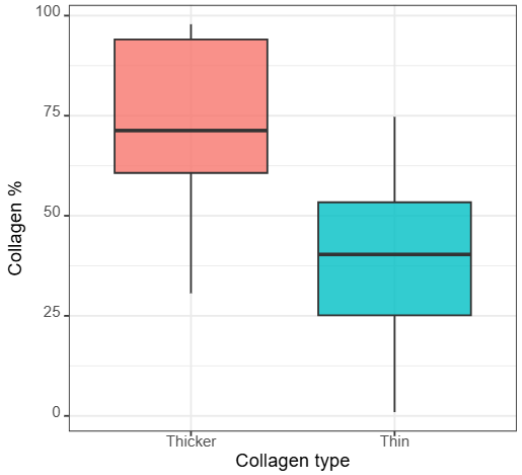

Figure 10. Box plot of the semi-quantitative analysis of collagen in the olfactory rosette of four specimens of *Scyliorhinus canicula*.

4. Discussion

This study demonstrated that analyzing the surface area of the secondary folds significantly increases the total surface area of the olfactory rosette, allowing for a more accurate estimation of olfactory capability than studies that only calculate the area of the primary lamellae. This occurs because the olfactory epithelium is organized into tightly packed sheets and further folded into secondary folds on both sides of each lamella, as previously described [31, 24, 36, 56]. Sensory and non-sensory epithelia can be easily distinguished, as they are characterized by different surface structures. The receptor cells that reach the apical surface possess only microvilli [58, 25, 31, 24].

In addition, a fixed number of primary lamellae was considered, since, as reported in previous studies, the number of lamellae in elasmobranchs remains relatively constant throughout growth [36, 59, 22]. This can be explained by the fact that fully developed organs at a young age may indicate that olfaction is an important sensory modality throughout all life stages [22].

Moreover, the non-uniform distribution of collagen due to water flow may support the idea proposed by [22], who measured raphe width and provided preliminary evidence that this parameter should be considered in future hydrodynamic studies. The raphe width, as a variable influencing hydrodynamic flow, suggests that regions containing more collagen are

those in greater contact with water, therefore requiring higher rigidity to withstand pressure, consistent with the observations made in this study.

With this work, it was possible to quantify the percentage increase in the sensory epithelium surface area of the olfactory organ of *Scyliorhinus canicula* promoted by secondary folds. The different staining techniques applied in this study also allowed the organization, structure, and characterization of the olfactory epithelium to be observed, showing that only a few regions consist of non-sensory tissue, such as those near the cartilaginous capsule and the raphe, while sensory tissue predominates throughout the organ.

5. Bibliographic references

[1] Hodgson, E. S. & Mathewson, R. F. (1978). Electrophysiological studies of chemoreception in elasmobranchs. *Sensory Biology of Sharks, Skates, and Rays*, 227-267.

[2] Kleerekoper, H. (1978). Chemoreception and its interaction with flow and light perception in the locomotion and orientation of some elasmobranchs. *Sensory Biology of Sharks, Skates, and Rays*, 269-329.

[3] Gardiner, J. M.; Hueter, R. E.; Maruska, K. P.; Sisneros, J. A.; Casper, B. M.; Mann, D. A. & Demski, L. S. (2012). Sensory physiology and behavior of elasmobranchs. *Biology of Sharks and their Relatives*, 1, 349-401.

[4] Collin, S. P.; Kempster, R. M. & Yopak, K. E. (2015). How elasmobranchs sense their environment. *Fish Physiology*, 34, 19-99.

[5] McEachran, J. D. & Aschliman, N. (2004). Phylogeny of batoidea. *Biology of Sharks and their Relatives*, 79-113.

[6] Musick, J. A.; Harbin, M. M. & Compagno, L. J. V. (2004). Historical zoogeography of the Selachii. *Biology of Sharks and their Relatives*, 1.

[7] Sims, D. W. (2010). Tracking and analysis techniques for understanding free-ranging shark movements and behavior. *Sharks and their Relatives II*, 367-408.

[8] Mayeur, H.; Leyhr, J.; Mulley, J.; Leurs, N.; Michel, L.; Sharma, K.; Lagadec, R.; Aury, J. M.; Osborne, O. G.; Mulhair, P.; Poulain, J.; Mangenot, S.; Mead, D.; Smith, M.; Corton, C.; Oliver, K.; Skelton, J.; Betteridge, E.; Dolucan, J.; Dudchenko, O.; Omer, A. D.; Weisz, D.; Aiden, E. L.; McCarthy, S.; Sims, Y.; Torrance, J.; Tracey, A.; Howe, K.; Baril, T.; Hayward, A.; Martinand-Mari, C.; Sanchez, S.; Haitina, T.; Martin, K.; Korsching, S. I.; Mazan, S. & Debias-Thibaud, M. (2024). The sensory shark: high-quality morphological, genomic and transcriptomic data for the small-spotted catshark *Scyliorhinus canicula* reveal the molecular bases of sensory organ evolution in jawed vertebrates. *Molecular Biology and Evolution*, 41(12).

[9] Shibuya, A.; Machado, R. N. & Duncan, W. P. (2024). Exploring the riverbed: how olfactory organ morphology shapes the life habits of freshwater stingrays (Potamotrygoninae). *Zoomorphology*, 143(3), 709-718.

[10] Montgomery, J. C. (1988) Sensory physiology. *Physiology of Elasmobranch Fishes*, 79-98.

[11] Tricas, T. C.; Kajiura, S. M. & Summers, A. P. (2009). Response of the hammerhead shark olfactory epithelium to amino acid stimuli. *Journal of Comparative Physiology A*, 195(10), 947-954.

[12] Hueter, R. E.; Mann, D. E.; Maruska, K. P.; Sisneros, J. A. & Demski, L. S. (2004). Sensory biology of elasmobranchs. *Biology of Sharks and Their Relatives*, 325–368.

[13] Meredith, T. L. & Kajiura, S. M. (2010). Olfactory morphology and physiology of elasmobranchs. *Journal of Experimental Biology*, 213(20), 3449-3456.

[14] Lisney, T. J. (2010). A review of the sensory biology of chimaeroid fishes (Chondrichthyes; Holocephali). *Reviews in Fish Biology and Fisheries*, 20(4), 571-590.

[15] Yopak, K. E.; Lisney, T. J. & Collin, S. P. (2015). Not all sharks are “swimming noses”: variation in olfactory bulb size in cartilaginous fishes. *Brain Structure and*

Function, 220(2), 1127-1143.

[16] Johnson, R. H. & Nelson, D. R. (1978). Copulation and possible olfaction-mediated pair formation in two species of carcharhinid sharks. *Copeia*, 1978(3), 539-542.

[17] Bullock, T. H. & Northcutt, R. G. (1984). Nervus terminalis in dogfish (*Squalus acanthias*, Elasmobranchii) carries tonic efferent impulses. *Neuroscience Letters*, 44(2), 155-160.

[18] Demski, L. S. & Northcutt, R. G. (1996). The brain and cranial nerves of the white shark: an evolutionary perspective. *Great White* Sharks, 121-130.

[19] Ferrando, S.; Gallus, L.; Ghigliotti, L.; Amaroli, A.; Abbas, G. & Vacchi, M. (2017). Clarification of the terminology of the olfactory lamellae in Chondrichthyes. *The Anatomical Record*, 300(11), 2039-2045.

[20] Hara, T. J. (1975). Olfaction in fish. *Progress in Neurobiology*, 5, 271-335.

[21] Hansen, A. & Zielinski, B. S. (2005). Diversity in the olfactory epithelium of bony fishes: development, lamellar arrangement, sensory neuron cell types and transduction components. *Journal of Neurocytology*, 34(3), 183-208.

[22] Clark, A.; Porter, M. & Meredith, T. L. (2022). Morphometric analysis of the elasmobranch olfactory rosette. *Journal of Morphology*, 283(11), 1464-1477.

[23] Tester, A. L. (1964). *Olfaction, Gustation, and the Common Chemical Sense in Sharks*.

[24] Theisen, B.; Zeiske, E. & Breucker, H. (1986). Functional morphology of the olfactory organs in the spiny dogfish (*Squalus acanthias* L.) and the small-spotted catshark (*Scyliorhinus canicula* (L.)). *Acta Zoologica*, 67(2), 73-86.

[25] Zeiske, E.; Theisen, B. & Gruber, S. H. (1987). Functional morphology of the olfactory organ of two carcharhinid shark species. *Canadian Journal of Zoology*, 65(10), 2406-2412.

[26] Abel, R. L.; Maclaine, J. S.; Cotton, R.; Xuan, V. B.; Nickels, T. B.; Clark, T. H.;

Wang, Z. & Cox, J. P. (2010). Functional morphology of the nasal region of a hammerhead shark. *Comparative Biochemistry and Physiology Part A: Molecular & Integrative Physiology*, 155(4), 464-475.

[27] Rygg, A. D.; Cox, J. P.; Abel, R.; Webb, A. G.; Smith, N. B. & Craven, B. A. (2013). A computational study of the hydrodynamics in the nasal region of a hammerhead shark (*Sphyrna tudes*): implications for olfaction. *PLoS One*, 8(3), e59783.

[28] Agbesi, M. P.; Naylor, S.; Perkins, E.; Borsuk, H. S.; Sykes, D.; Maclaine, J. S.; Wang, Z. & Cox, J. P. (2016). Complex flow in the nasal region of guitarfishes. *Comparative Biochemistry and Physiology Part A: Molecular & Integrative Physiology*, 193, 52-63.

[29] Kajiura, S. M.; Forni, J. B. & Summers, A. P. (2005). Olfactory morphology of carcharhinid and sphyrnid sharks: does the cephalofoil confer a sensory advantage? *Journal of Morphology*, 264(3), 253-263.

[30] Faucette, J. R. (1969). The olfactory bulb and medial hemisphere wall of the rat-fish, Chimaera. *Journal of Comparative Neurology*, 137(4), 377-405.

[31] Holl, A. (1973). Feinstruktur des riechepithels von *Chimaera monstrosa* (Holocephali). *Marine Biology*, 23(1), 59-72.

[32] Meng, Q. & Yin, M. (1981). A study of the olfactory organ of the sharks. *Transactions of the Chinese Ichthyological Society*, 2, 1-24.

[33] Meng, Q. & Yin, M. (1981). A study on the olfactory organ of skates, rays and chimaeras. *Journal of Fisheries of China*, 5(3), 209-228.

[34] Bell, M. A. (1993). Convergent evolution of nasal structure in sedentary elasmobranchs. *Copeia*, 144-158.

[35] Fishelson, L. & Baranes, A. (1997). Ontogenesis and cytomorphology of the nasal olfactory organs in the Oman shark, *Iago omanensis* (Triakidae), in the Gulf of Aqaba, Red

Sea. *The Anatomical Record: An Official Publication of the American Association of Anatomists*, 249(3), 409-421.

[36] Schluessel, V.; Bennett, M. B.; Bleckmann, H.; Blomberg, S. & Collin, S. P. (2008). Morphometric and ultrastructural comparison of the olfactory system in elasmobranchs: the significance of structure–function relationships based on phylogeny and ecology. *Journal of Morphology*, 269(11), 1365-1386.

[37] Theiss, S. M.; Hart, N. S. & Collin, S. P. (2009). Morphological indicators of olfactory capability in wobbegong sharks (Orectolobidae, Elasmobranchii). *Brain Behavior and Evolution*, 73(2), 91-101.

[38] Timm, L. L. & Fish, F. E. (2012). A comparative morphological study of head shape and olfactory cavities of sharks inhabiting benthic and coastal/pelagic environments. *Journal of Experimental Marine Biology and Ecology*, 414, 75-84.

[39] Yamamoto, M. (1982). Comparative morphology of the peripheral olfactory organ in teleosts. *Chemoreception in fishes*, 39-59.

[40] Cox, J. P. (2008). Hydrodynamic aspects of fish olfaction. *Journal of the Royal Society Interface*, 5(23), 575-593.

[41] Springer, S. (1979). A revision of the catsharks, family Scyliorhinidae. *National Oceanic and Atmospheric Administration, National Marine Fisheries Service*, 55.

[42] Rodríguez-Cabello, C.; Sánchez, F. & Olaso, I. (2007). Distribution patterns and sexual segregations of *Scyliorhinus canicula* (L.) in the Cantabrian Sea. *Journal of Fish Biology*, 70(5), 1568-1586.

[43] Wheeler, A. (1969). The fishes of the British Isles and north west Europe.

[44] Wheeler, A. (1978). Key to the fishes of northern Europe: a guide to the identification of more than 350 species.

[45] Compagno, L. J. (2001). Sharks of the world: an annotated and illustrated catalogue of shark species known to date, 1. *Food & Agriculture Org.*

[46] Sánchez, F. (1993). Las comunidades de peces de la plataforma del Cantábrico. *Centro Oceanográfico de Santander*.

[47] Sánchez, F.; Blanco, M. & Gancedo, R. M. (2002). Atlas de los peces demersales y de los invertebrados de interés comercial de Galicia y el Cantábrico. Otoño 1997-1999.

[48] Rodrıguez-Cabello, C.; Sánchez, F.; Fernández, A. & Olaso, I. (2004). Is the lesser spotted dogfish (*Scyliorhinus canicula*) population from the Cantabrian Sea a unique stock? *Fisheries research*, 69(1), 57-71.

[49] Smith, L. E. (2018). Plastic ingestion by *Scyliorhinus canicula* trawl captured in the North Sea. *Marine pollution bulletin*, 130, 6-7.

[50] Wheeler, A. (1978). Key to the fishes of northern Europe: a guide to the identification of more than 350 species.

[51] Ellis, J. R. & Shackley, S. E. (1997). The reproductive biology of *Scyliorhinus canicula* in the Bristol Channel, UK. *Journal of Fish Biology*, 51(2), 361-372.

[52] Ferrando, S.; Gallus, L.; Ghigliotti, L.; Vacchi, M.; Nielsen, J.; Christiansen, J. S. & Pisano, E. (2016). Gross morphology and histology of the olfactory organ of the Greenland shark *Somniosus microcephalus*. *Polar Biology*, 39(8), 1399-1409.

[53] Ferrando, S.; Gallus, L.; Ghigliotti, L.; Vacchi, M.; Amaroli, A.; Nielsen, J. & Pisano, E. (2017). Anatomy of the olfactory bulb in Greenland shark *Somniosus microcephalus* (Bloch & Schneider, 1801). *Journal of Applied Ichthyology*, 33(2), 263-269.

[54] Rasband, W. S. (1997–2014). ImageJ. Bethesda: National Institutes of Health.

[55] Abràmoff, M. D.; Magalhães, P. J. & Ram, S. J. (2004). Image processing with ImageJ. *Biophotonics international*, 11(7), 36-42.

[56] Ferrando, S.; Amaroli, A.; Gallus, L.; Aicardi, S.; Di Blasi, D.; Christiansen, J. S. & Ghigliotti, L. (2019). Secondary folds contribute significantly to the total surface area in the olfactory organ of Chondrichthyes. *Frontiers in Physiology*, 10, 245.

[57] Reese, T. S. & Brightman, M. W. (1970). Olfactory surface and central olfactory connexions in some vertebrates. *Ciba Foundation Symposium-Internal Secretions of the Pancreas (Colloquia on Endocrinology)*, 115-149.

[58] Zeiske, E.; Caprio, J. & Gruber, S. H. (1986). Morphological and electrophysiological studies on the olfactory organ of the lemon shark, *Negaprion brevirostris*. *Indo-Pacific Fish Biology: Proceedings of the Second International Conference on Indo-Pacific Fishes*, 381-391.

[59] Schluessel, V.; Bennett, M. B.; Bleckmann, H. & Collin, S. P. (2010). The role of olfaction throughout juvenile development: functional adaptations in elasmobranchs. *Journal of morphology*, 271(4), 451-461.

UNIVERSIDADE ESTADUAL PAULISTA
"JÚLIO DE MESQUITA FILHO"
Instituto de Biociências
Câmpus do Litoral Paulista

PARECER FINAL DO TRABALHO DE CONCLUSÃO DE CURSO

Discente: LUISA TROVATTI CUSTÓDIO

Título: *"Morfologia e histologia da roseta olfatória do tubarão-gato, Scyliorhinus canicula (Chondrichthyes, Scyliorhinidae)"*

Orientador: Prof. Dr. Otto Bismarck Fazzano Gadig

Curso/Habilitação: Bacharelado em Ciências Biológicas/Gerenciamento Costeiro

COMISSÃO EXAMINADORA	CONCEITO
Prof. Dr. Otto Bismarck Fazzano Gadig	APROVADO
Prof. Dr. Ivan Sergio Nunes Silva Filho	APROVADO

PARECER:
TRABALHO APRESENTADO COM CLAREZA E SEGURANÇA NA DEFESA. A QUALIDADE DO ESTUDO ESTUDO É ALTA, COM TEMA QUE SE MOSTROU INOVADOR. A ALUNA TEM GRANDE MÉRITO E DEVE RECEBER O SEU TÍTULO DE BIÓLOGA. PARABÉNS PARA ELA E SEUS ORIENTADORES.

CONCEITO FINAL:

A Comissão Examinadora abaixo assinada conclui que a discente **Luisa Trovatti Custódio** obteve o seguinte conceito:

☒ APROVADO ☐ REPROVADO

São Vicente, 30 de junho de 2026.

Prof. Dr. Otto Bismarck Fazzano Gadig

Prof. Dr. Ivan Sergio Nunes Silva Filho

Instituto de Biociências - Câmpus do Litoral Paulista
Praça Infante D. Henrique s/nº - CEP 11330-900 - São Vicente (SP) - Brasil
Tel. (13) 3569-7100 - diretor.clp@unesp.br